The impacts of irrigation on California's simulated climate by the variable-resolution CESM

Xingying Huang,[1] Paul A. Ullrich,[1]

add abstract

1. Introduction

Over the past century, human activity has strongly impacted the climate both globally and regionally, largely through impacts associated with increasing greenhouse gases [*Solomon*, 2007], but also as a result of land cover changes, particularly deforestation and urbanization [*Bonan*, 1997; *Pielke et al.*, 2002; *Kueppers et al.*, 2008]. Conversion of the natural land surface to cropland features prominently in this change, which is accompanied by modified albedo and changes to both sensible and latent heat fluxes [*Foley et al.*, 2003]. Additionally, besides changes to energy balance, land management also plays a important role in affecting the climate by modifying the carbon and water cycles, which are impacted by cropping length and irrigation strategy [*Lobell et al.*, 2006]. The pronounced cooling effect by irrigation, especially over regions where irrigation is extensive, has already been emphasized by previous studies [*Kueppers et al.*, 2007; *Lobell and Bonfils*, 2008].

California is the most irrigated state in the United States, and most of California's irrigated cropland is distributed over the Central Valley (CV), which is in turn responsible for 25% of the agricultural products in the U.S. [*Wilkinson et al.*, 2002]. The CV extends 600 km between its northernmost and southernmost point and is between 60-100km in width. It features a vast agricultural industry that has adapted to an extremely dry growing season within its the Mediterranean climate through the adoption of extensive irrigation practices. The USGS reports that in the year 2000, approximately 42 km^3 of water was used over 41,000 km^2 of irrigated area within California [*Döll and Siebert*, 2002; *Famiglietti et al.*, 2011]. As a result, *Bonfils and Lobell* [2007] found that irrigation over CV has decreased summertime maximum temperature by ∼2-3 K in heavily-irrigated areas compared with nearby non-irrigated areas, based on long-term temperature records, although these impacts have had a negligible effect on nighttime temperatures. Similar impacts have also been demonstrated in Nebraska's irrigated areas by [*Mahmood et al.*, 2006].

However, irrigation effects are usually ignored in climate models for several reasons: irrigation usually occurs over a relatively small area (∼2% of global land surface) and produces a seemingly negligible cooling effect compared to global greenhouse warming [*Boucher et al.*, 2004]. Nonetheless, with the increasing need for more accurate regional climate studies, irrigation practices are a potentially important factor in regulating the climate patterns of heavily irrigated regions. Consequently, the climatic effects of irrigation have been assessed in limited-area models (LAMs) [*Snyder et al.*, 2006; *Kueppers et al.*, 2007] (in the context of climate modeling, LAMs are typically referred to as regional climate models (RCMs)). In these studies, irrigation was modeled by account for the amount of irrigated water needed and the area of cropland where irrigation is applied. Based on simulations by the different RCMs, *Kueppers et al.* [2008] compared the effects of irrigation on regional climate, and found that behaviors of RCMs varied, depending on each models physics, as well as on irrigation configurations.

Although global climate models (GCMs) rarely account for irrigation, it is nonetheless meaningful to understand to what extent irrigation may affect the global climate patterns. *Lobell et al.* [2006] coupled the community atmosphere model (CAM v3.0) to the community land model (CLM) 3.0 at ∼2-2.5° horizontal grid spacing to model irrigation by fixing soil moisture at saturation during the growing season in all croplands. Although this approach likely overcompensated for total added water, his results estimated that global irrigation led to a global land surface cooling of 1.3 K, and regional cooling of up to 8 K. *Lo and Famiglietti* [2013] used CAM 3.5 along with the community land model (CLM v3.5) at ∼1.4°, and showed that the increase in evapotranspiration and water vapor due to irrigation significantly impacts the atmospheric circulation in the southwestern United States with strengthening the regional hydrological cycle.

Aforementioned studies that addressed the impact of irrigation either used RCMs or coarse-resolution GCMs along with different irrigation schemes. In order to model regional climate over the CV, relatively fine horizontal resolution is needed to more accurately represent microclimates, land-use, small-scale dynamical features and interactions so as to address local needs in formulating climate adaptation and mitigation strategies [*Leung et al.*, 2003; *Rauscher et al.*, 2010]. In this paper, we use the recently developed variable-resolution option in Community Earth System Model (VR-CESM) to study the impact of irrigation on regional climate over the CV, using a more flexible irrigation scheme with relatively realistic estimates of regional agricultural water use (as will be described in Section 2). Variable-resolution GCMs (VRGCMs) such as VR-CESM use a relatively coarse global model with enhanced resolution over a specific region [*Staniforth and Mitchell*, 1978; *Fox-Rabinovitz et al.*, 1997]. Compared with RCMs, a key advantage of VRGCMs is that they use a single, unified modeling framework, rather than a separate GCM and RCM with potentially inconsistent dynamics and physics parameterizations and lack of two-way interactions at the nest boundary [*Laprise et al.*, 2008]. Compared to uniform-resolution global models, VRGCMs provide a cost-effective approach for reaching high resolutions over a region of interest – the regional simulations in this study at ∼28 km resolution represent a reduction in required computation of approximately 10 times over a global uniform resolution 0.25° simulation. VR-CESM has been demonstrated to be effective for regional climate studies and applications at a reduced computational cost compared to uniform GCMs [*Zarzycki et al.*, 2015; *Rhoades et al.*, 2015]. This study represents the first time variable resolution has been used to assess a parameterization in a global modeling system.

[1]Department of Land, Air and Water Resources, University of California, Davis

0094-8276/15/$5.00

This study applies the irrigation option in CLM 4.0 coupled in CESM 1.2.0 to investigate the impact of irrigation not only on mean climatology, but also on heat extremes over recently past climate from year 1980-01-01 to 2005-12-31 in the CV. This paper is organized as follows: Section 2 describes the model setup, employed datasets and methodology. In section 3, simulation results are provided and discussed. Key results are summarized along with further discussion in section 4.

2. Model setup and reference datasets

2.1. Irrigation scheme

As a state-of-the-art Earth modeling framework, CESM 1.2.0 consists of coupled atmospheric, oceanic, land and sea ice models [*Neale et al.*, 2010a; *Hurrell et al.*, 2013]. In this study, CAM version 5 (CAM5) [*Neale et al.*, 2010b] and the Community Land Model (CLM) version 4.0 [*Oleson et al.*, 2010a] are used. The finest horizontal resolution of our grid is 0.25 ° (∼ 28km) covering the western U.S., with a quasi-uniform 1 ° mesh over the remainder of the globe. Considering the relatively flat topography (less than 100m) over most of CV, the ∼ 28km grid resolution satisfies our need for modeling irrigation effects. Detailed descriptions of VR-CESM employed in this paper can be found in *Rhoades et al.* [2015], here, we only focus on the irrigation scheme within CLM 4.0. Include a picture of the mesh being employed

The irrigation model we use is described in *Sacks et al.* [2009]. The fractional area of the cropland within each grid cell (independent of specific type) that is equipped for irrigation is from *Siebert et al.* [2005, 2007] for the year 2000, and is fixed over the simulation period (see Figure 1). This assumption is reasonable since irrigated area has been largely unchanged in California since 1980 [*Bonfils and Lobell*, 2007].

The need for daily irrigation is determined at 6 AM local time by computing the deficit between the current soil moisture content and a target soil moisture content. If positive, the difference is then added to the ground surface at a constant rate over the following four hours, bypassing canopy interception. By default, CLM simulates ten soil layers, with a total depth of 3.4 m [*Oleson et al.*, 2010b]. The target soil moisture content in each soil layer i ($w_{target,i}$, in kg/m^2) is a weighted average of (a) the minimum soil moisture content that results in no water stress ($w_{o,i}$, kg/m^2) and (b) the soil moisture content at saturation ($w_{sat,i}$, kg/m^2) [*Oleson et al.*, 2010b], in accordance with

$$w_{target,i} = (1 - \alpha) * w_{o,i} + \alpha * w_{sat,i}. \tag{1}$$

The default value of the irrigation weight factor α is 0.7, which was determined empirically to give global, annual irrigation amounts that approximately match observed gross irrigation water use around the year 2000 [*Shiklomanov*, 2000]. More details about the irrigation model can be found in the online technical description (`http://www.cesm.ucar.edu/models/cesm1.2/clm/`). [This should probably be a citation rather than a URL]

2.2. Simulations

In order to understand the impacts on the local climate triggered by irrigation of the CV, we have conducted a control run (NRG) without irrigation and two irrigation-enabled runs, referred to as IRG and IRG(0.5) respectively. The IRG run uses the default irrigation weight factor $\alpha = 0.7$. This value was adjusted to 0.5 in the IRG(0.5) run so as to determine the impact of changes in total irrigated water. Both simulations were performed over the period 1979-01-02 to 2005-12-31 (UTC). For purposes of analysis, 1979 was discarded as a spin-up period. The 26-year time period was chosen to provide an adequate sampling of annual variability within computational constraints.

For the NRG run, we used a 0.5 ° resolution land cover dataset, fixed at year 2000. After this simulation was completed, a finer land cover dataset at 3min (∼ 10 km) was obtained that provided a more realistic fraction of irrigated cropland in each grid cell over the CV. After interpolation to the variable-resolution model grid, the only other significant difference between datasets was 10-20% more c3 non-arctic grass in the study region, which we determined did not impact the local climatology. Consequently, the higher resolution dataset was employed for both IRG simulations.

3. Methodology

In the CV, irrigation peaks during the summer growing season [*Salas et al.*, 2006] in response to California's dry Mediterranean summers [add observation values here]. Our simulations accurately reproduce this result, as most irrigated water is added during summer (see supplement document [explain what info is in the supplement]). To study the climatological impacts of irrigation, we focus primarily on changes in June, July and August (JJA) near-surface temperatures due to irrigation, and the associated mechanisms driving this change. The variables of interest for this study are daily maximum, minimum and average 2m temperatures (Tmax, Tmin and Tavg).

To determine how irrigation affects heat extremes within the CV, we calculated the hot spell length, hot spell frequency, and mean Tmax over the hot spells. For our purposes, a hot spell is defined as at least five consecutive days when Tmax exceeds 38°C. This threshold value approximately corresponds to the 90th percentile of the daily JJA Tmax over the 1980-2005 period within the CV. *Hot spell length* is defined as the average duration (in days) for all hot spells over the 26 year period, *hot spell frequency* is defined as the average number of hot spells per year, and *mean hot spell Tmax* is defined as the average Tmax over all the hot spell days. When analyzing hot spells, declustering is employed following the strategy of *Ferro and Segers* [2003] to ensure hot spells are serially independent. This functionality is implemented in the R package `extReme` [*Gilleland and Katz*, 2011].

Simulation results were not detrended since the linear trend was small [Define small]. To restrict the analysis to the CV, the variables of interest have been masked and/or averaged within the area defined by the bounded region depicted in Figure 1, which contains 155 degrees of freedom.

add info for supplement: Complementary results to this study are provided in the online supplement, including the xxx.

3.1. Reference datasets

For comparison, we employ two high-quality gridded observational datasets (UW and PRISM) and selected weather station data to evaluate our simulation output. The detailed descriptions of these reference datasets are as follows.

UW:: The UW daily gridded meteorological data is obtained from the Surface Water Modeling group at the University of Washington [*Maurer et al.*, 2002; *Hamlet and Lettenmaier*, 2005]. The dataset is provided at 0.125° horizontal resolution covering the period from year 1949 to 2010 with daily time frequency. This study used variables Tmax and Tmin from the dataset.

PRISM:: The Parameter-elevation Regressions on Independent Slopes Model (PRISM) [*Daly et al.*, 2008] 4 km gridded dataset is also employed in this study. This model ingests point measurements and applies a weighted regression scheme that accounts for key factors affecting the local climatology. PRISM is the United States Department of Agriculture's official climatological dataset. Monthly climatological variables are available for 1895 through 2015 and daily data for 1981 to 2015 from the PRISM Climate Group (Oregon State University, http://prism.oregonstate.edu, created 4 Feb 2004) [A citation is better than a URL]. This study makes use of monthly Tmax, Tmin, Tavg, and daily Tmax.

NCDC:: Weather station measurements over the CV are obtained from the Global Historical Climate Network (GHCN) and provided by NOAA/NCDC, http://www.ncdc.noaa.gov/ [Citation better than URL]). An even distribution of weather stations within the study region was chosen from all stations with at least 90% observations of Tmax and Tmin over all JJA days from 1980 to 2005. Consequently, approximately 20 weather stations were employed for recorded Tmax and Tmin.

4. Results

The average JJA Tmin, Tavg and Tmax over the 1980-2005 time period from all simulations and gridded datasets is depicted in Figure 2. Relative to the gridded datasets, it can be seen that NRG has a prominent overestimation of Tmax, with MSD [define in text, not caption] values of ∼1 K and RMSD [define in text, not caption] values of ∼1.8 K (see Table 1). The cooling effect caused by irrigation can be clear seen in the Tmax field when comparing NRG and IRG results. Notably, no clear difference in temperatures arises from reducing the irrigation factor from 0.7 to 0.5. Although the IRG run shows a slight cold bias with an MSD of ∼ -0.36 K (which is slightly reduced in IRG(0.5) to ∼ -0.2 K), this effect is limited to the base of the Sierra Nevada and the Delta region. Compared with NRG, the RMSD of Tmax is only reduced by about 20%, which appears to be due to the offset effects caused by the non-irrigated grid cells around our study region's boundary. Tmin is almost the same for all three runs, showing a slight warm bias relative to UW and PRISM. The net result was that Tavg was overestimated in NRG over the CV, except in regions influenced by the Delta sea breeze. On the other hand, IRG showed a slight cool bias in Tavg after alleviating the overestimation of Tmax in the northern and southern reaches of the CV. Over non-irrigated area, the results are almost the same for all the runs, suggesting that temperature modulation is largely a local phenomenon. Note that UW and PRISM Tmax fields are statistically identical in the CV.

In order to further figure out the potential underlying processes related with irrigation, we have looked into multiple relevant variables as summed in Table 2. Under irrigation, the specific humidity has increased about 15% and the sensible heat flux has decreased 16% mainly along with the cooler surface. Due to the scarcity of precipitation (∼0.1 mm/day) and extreme hot summer over CV, the latent heat flux has largely increased for about 71% after adding ∼1.27 mm/day irrigated water for IRG(0.5), as further shown in Figure 3. Ground evaporation is positively related with latent heat flux. The average soil moisture over all the subsurface layers has only increased a little (∼ 5%) under irrigation, but this increase is significant according the T-test result (also see Figure 3). Although the irrigated water of IRG(0.5) is nearly half of what for IRG, they did not show notable differences for those variables, which explains the similar results of the near surface temperatures from these two irrigation runs as we discussed above. The possible reason may due to abnormally large surface runoff (∼1.6 mm/day) for IRG0.7 comparing with IRG0.5 (∼0.24 mm/day) .

We have also investigated the relationships among relevant variables based on the JJA values over 26 years to see if the land surface model works reasonably with irrigation. It turned out that, for IRG(0.5) irrigated water is positively correlated with soil moisture, however, this does not hold for IRG. And latent heat flux is positively correlated with soil moisture especially for IRG(0.5) and NRG. Tmax is positively correlated with irrigated water for in IRG(0.5) run but not correlated with soil moisture or latent heat flux. (add correlation coefficients here The boxplot in Figure 3 showed that both the average magnitude and variability of Tmax has been improved with irrigation. Though average precipitation did not differ among these three runs, adding irrigation tends to widen the distribution of precipitation intensity and bring more extreme precipitation occurrences. (say more about this box plot)

add how the surface runoff is produced

Since hot spells dominate during the summer season over CV, the frequency distribution of Tmax using all JJA daily values at each grid point over year 1981-2005 is depicted for all the runs and reference datasets including UW, PRISM and 21 weather stations (with area weight) in Figure 4. As we can see, the NRG run exhibited a clear warm bias associated with a long forward upper tail with maximum temperatures approaching near 50 °C. Compared with NRG, irrigation runs displayed much closer distribution to UW and PRISM, especially over the upper bound, though some colder bias is existed between lower bound and upper bound. Overall, though irrigation runs captures the general distribution of Tmax, they are not so skewed to left and have more flat peaks than observations as told by the moments in Table 3.

The hot spell features derived from of the simulations and UW dataset (PRISM is similar to UW, not shown) are tabulated in Table 4. We can see that, with irrigation, the simulations satisfactorily captured the hot spell features with close values to observations. Due to the cooling effect of irrigation, the duration and number of hot spells averaged over each year have both reduced about 30% comparing to the NRG run. The mean Tmax over hot spell between IRG and NRG did not show higher magnitude of difference than the average Tmax over JJA as above talked, and is around 40°C, which is 2°C higher than the threshold. This behavior that irrigation did not show larger effects on hot days than average summer day has also been observed by *Lobell et al.* [2008].

Due to the important role CV plays in agricultural industry, we have also looked at the heat stress for crops. We calculated the hours that exceeding a threshold over each day of JJA based on the hourly outputs from year 2000 (only this year has hourly output) and averaged the value over CV area. Here we chose 35 °C to be our threshold as used in *Teixeira et al.* [2013]. As Figure 5 showed, both the heat stress intensity and frequency have reduced under irrigation. The average hours over all days in this JJA are 2.152 for NRG and 1.424 for IRG (about 34% less).

5. Discussion and Summary

With irrigation, the nighttime warming can occur and daily Tmin can increase due to the increased thermal conductivity of wet soil found by *Kanamaru and Kanamitsu* [2008], or with increased heat capacity of the soil and vegetation as argued by *Bonfils and Lobell* [2007], over CV. However, in our irrigation runs, Tmin did not really change, since the soil moisture only increased for about 5% comparing with non-irrigated one and did not result in notable nighttime warming.

Lo and Famiglietti [2013] found that the irrigation in the Central Valley results in higher precipitation rates (∼15%) over the southwestern U.S., together with enhancing summer monsoon rainfall. In our study, the specific humidity do showed statistically significant increase for about 15% over irrigated area, and this increase also occurred over southern California (see Figure 6), though, precipitation did not really enlarge (for about %10, but not statistically significant). This gives another evidence that irrigation in the Central Valley could change the regional hydrological cycle with water vapor transport, by modifying the depths of planetary boundary layer, lifting condensation level and mixing layer [*Segal et al.*, 1998; *Adegoke et al.*, 2003; *DeAngelis et al.*, 2010; *Qian et al.*, 2013].

As we showed, the irrigated water in IRG run is 2.838 mm/day in JJA averaged over CV, and this equals to 31.7 km^3 water in total. As we mentioned in the introduction part that, in year 2000, USGS reported about 42 km^3 of water is used over 41,000 km^2 of irrigated area in California. Assuming half to two thirds of the 42 km^3 of water is employed over CV during JJA, and that is about 21 to 28 km^3, which is nearly 0.66 to 0.88 times the amount put in the irrigation simulation. However, the irrigation scheme in CLM4.0 for our study can adjust the water deficit according to the actual soil moisture, and by assigning different irrigation weights, irrigated water can be increased or reduced accordingly, as similarly investigated by [*Leng et al.*, 2013]. However, in the model, intensified irrigation did not result in notable wetter soil or enhanced latent heat flux, but increased surface runoff. And we also did five years' test run with reduced irrigation weight factor largely to 0.1, and results are still similar to the IRG run which has ∼3.4 times more irrigated water. Then we changed the irrigation factor to zero, and added half of the water that calculated from the deficit equation described in Section 2, with the irrigated water amount of 0.42 mm/day. With five years' test run, we got the average latent heat flux around 50.66 W/m^2, which is about 80% of the value of IRG run. Therefore, when more irrigation water is added, the latent heat flux will be enhanced, and the soil moisture will increase. However, once the irrigated water amount is larger than a specific level, the latent heat flux will become quite stable, and extra water will further infiltrate to the soil. However, if the irrigated water keeps increasing to a relative high level, most of the extra water will result into surface runoff rather than groundwater. It seems that the CLM model performs relatively conservatively in soil moisture regulation. And since CLM does not simulate subsurface flow which is taken care by independent watershed model, it lacks realistic control of water infiltration configurations or ground water replenish efficiency.

With current intense drought, over-pumping groundwater would result in more and more dry soil. And irrigation-induced cooling could be slowdown, which makes the Central Valley even more vulnerable to future greenhouse-induced warming [*Bonfils and Lobell*, 2007; *Williams et al.*, 2015].

add summary

add future work

Acknowledgments.

References

Adegoke, J. O., R. A. Pielke Sr, J. Eastman, R. Mahmood, and K. G. Hubbard (2003), Impact of irrigation on midsummer surface fluxes and temperature under dry synoptic conditions: A regional atmospheric model study of the us high plains, *Monthly Weather Review*, *131*(3), 556–564.

Bonan, G. B. (1997), Effects of land use on the climate of the united states, *Climatic Change*, *37*(3), 449–486.

Bonfils, C., and D. Lobell (2007), Empirical evidence for a recent slowdown in irrigation-induced cooling, *Proceedings of the National Academy of Sciences*, *104*(34), 13,582–13,587.

Boucher, O., G. Myhre, and A. Myhre (2004), Direct human influence of irrigation on atmospheric water vapour and climate, *Climate Dynamics*, *22*(6-7), 597–603.

Daly, C., M. Halbleib, J. I. Smith, W. P. Gibson, M. K. Doggett, G. H. Taylor, J. Curtis, and P. P. Pasteris (2008), Physiographically sensitive mapping of climatological temperature and precipitation across the conterminous United States, *International Journal of Climatology*, *28*(15), 2031–2064.

DeAngelis, A., F. Dominguez, Y. Fan, A. Robock, M. D. Kustu, and D. Robinson (2010), Evidence of enhanced precipitation due to irrigation over the great plains of the united states, *Journal of Geophysical Research: Atmospheres (1984–2012)*, *115*(D15).

Döll, P., and S. Siebert (2002), Global modeling of irrigation water requirements, *Water Resources Research*, *38*(4), 8–1.

Famiglietti, J., M. Lo, S. Ho, J. Bethune, K. Anderson, T. Syed, S. Swenson, C. de Linage, and M. Rodell (2011), Satellites measure recent rates of groundwater depletion in california's central valley, *Geophysical Research Letters*, *38*(3).

Ferro, C. A., and J. Segers (2003), Inference for clusters of extreme values, *Journal of the Royal Statistical Society: Series B (Statistical Methodology)*, *65*(2), 545–556.

Foley, J. A., M. H. Costa, C. Delire, N. Ramankutty, and P. Snyder (2003), Green surprise? how terrestrial ecosystems could affect earth's climate, *Frontiers in Ecology and the Environment*, *1*(1), 38–44.

Fox-Rabinovitz, M. S., G. L. Stenchikov, M. J. Suarez, and L. L. Takacs (1997), A finite-difference GCM dynamical core with a variable-resolution stretched grid, *Monthly Weather Review*, *125*(11), 2943–2968.

Gilleland, E., and R. W. Katz (2011), New software to analyze how extremes change over time, *Eos, Transactions American Geophysical Union*, *92*(2), 13–14.

Hamlet, A. F., and D. P. Lettenmaier (2005), Production of Temporally Consistent Gridded Precipitation and Temperature Fields for the Continental United States*, *Journal of Hydrometeorology*, *6*(3), 330–336.

Hurrell, J. W., M. M. Holland, P. R. Gent, S. Ghan, J. E. Kay, P. Kushner, J.-F. Lamarque, W. G. Large, D. Lawrence, K. Lindsay, et al. (2013), The community earth system model: A framework for collaborative research, *Bulletin of the American Meteorological Society*, *94*(9), 1339–1360.

Kanamaru, H., and M. Kanamitsu (2008), Model diagnosis of nighttime minimum temperature warming during summer due to irrigation in the california central valley, *Journal of Hydrometeorology*, *9*(5), 1061–1072.

Kueppers, L. M., M. A. Snyder, and L. C. Sloan (2007), Irrigation cooling effect: Regional climate forcing by land-use change, *Geophysical Research Letters*, *34*(3).

Kueppers, L. M., M. A. Snyder, L. C. Sloan, D. Cayan, J. Jin, H. Kanamaru, M. Kanamitsu, N. L. Miller, M. Tyree, H. Du, et al. (2008), Seasonal temperature responses to land-use change in the western united states, *Global and Planetary Change*, *60*(3), 250–264.

Laprise, R., R. De Elia, D. Caya, S. Biner, P. Lucas-Picher, E. Diaconescu, M. Leduc, A. Alexandru, and L. Separovic (2008), Challenging some tenets of regional climate modelling, *Meteorology and Atmospheric Physics*, *100*(1-4), 3–22.

Leng, G., M. Huang, Q. Tang, W. J. Sacks, H. Lei, and L. R. Leung (2013), Modeling the effects of irrigation on land surface fluxes and states over the conterminous united states: Sensitivity to input data and model parameters, *Journal of Geophysical Research: Atmospheres*, *118*(17), 9789–9803.

Leung, L. R., L. O. Mearns, F. Giorgi, and R. L. Wilby (2003), Regional climate research: needs and opportunities, *Bulletin of the American Meteorological Society*, *84*(1), 89–95.

Lo, M.-H., and J. S. Famiglietti (2013), Irrigation in california's central valley strengthens the southwestern us water cycle, *Geophysical Research Letters*, *40*(2), 301–306.

Lobell, D., G. Bala, and P. Duffy (2006), Biogeophysical impacts of cropland management changes on climate, *Geophysical Research Letters*, *33*(6).

Lobell, D. B., and C. Bonfils (2008), The effect of irrigation on regional temperatures: A spatial and temporal analysis of trends in california, 1934-2002, *Journal of Climate*, *21*(10), 2063–2071.

Lobell, D. B., C. J. Bonfils, L. M. Kueppers, and M. A. Snyder (2008), Irrigation cooling effect on temperature and heat index extremes, *Geophysical Research Letters*, *35*(9).

Mahmood, R., S. A. Foster, T. Keeling, K. G. Hubbard, C. Carlson, and R. Leeper (2006), Impacts of irrigation on 20th century temperature in the northern great plains, *Global and Planetary Change*, *54*(1), 1–18.

Maurer, E., A. Wood, J. Adam, D. Lettenmaier, and B. Nijssen (2002), A long-term hydrologically based dataset of land surface fluxes and states for the conterminous United States*, *Journal of climate*, *15*(22), 3237–3251.

Neale, R. B., C.-C. Chen, A. Gettelman, P. H. Lauritzen, S. Park, D. L. Williamson, A. J. Conley, R. Garcia, D. Kinnison, J.-F. Lamarque, et al. (2010a), Description of the NCAR community atmosphere model (CAM 5.0), *NCAR Tech. Note NCAR/TN-486+ STR*.

Neale, R. B., C.-C. Chen, A. Gettelman, P. H. Lauritzen, S. Park, D. L. Williamson, A. J. Conley, R. Garcia, D. Kinnison, J.-F. Lamarque, D. Marsh, M. Mills, A. K. Smith, S. Tilmes, F. Vitt, P. Cameron-Smith, W. D. Collins, M. J. Iacono, , R. C. Easter, X. Liu, S. J. Ghan, P. J. Rasch, and M. A. Taylor (2010b), Description of the NCAR Community Atmosphere Model (CAM 5.0), *NCAR Technical Note NCAR/TN-486+STR*, National Center for Atmospheric Research, Boulder, Colorado.

Oleson, K., D. Lawrence, G. Bonan, M. Flanner, E. Kluzek, P. Lawrence, S. Levis, S. Swenson, P. Thornton, A. Dai, M. Decker, R. Dickinson, J. Feddema, C. Heald, F. Hoffman, J. Lamarque, N. Mahowald, G. Niu, T. Qian, J. Randerson, S. Running, K. Sakaguchi, A. Slater, R. Stockli, A. Wang, Z. Yang, X. Zeng, and X. Zeng (2010a), Technical description of version 4.0 of the Community Land Model (CLM), *NCAR Technical Note NCAR/TN-478+STR*, National Center for Atmospheric Research, Boulder, Colorado, doi:10.5065/D6FB50WZ.

Oleson, K. W., D. M. Lawrence, B. Gordon, M. G. Flanner, E. Kluzek, J. Peter, S. Levis, S. C. Swenson, E. Thornton, J. Feddema, et al. (2010b), Technical description of version 4.0 of the community land model (clm).

Pielke, R. A., G. Marland, R. A. Betts, T. N. Chase, J. L. Eastman, J. O. Niles, S. W. Running, et al. (2002), The influence of land-use change and landscape dynamics on the climate system: relevance to climate-change policy beyond the radiative effect of greenhouse gases, *Philosophical Transactions of the Royal Society of London A: Mathematical, Physical and Engineering Sciences*, *360*(1797), 1705–1719.

Qian, Y., M. Huang, B. Yang, and L. K. Berg (2013), A modeling study of irrigation effects on surface fluxes and land–air–cloud interactions in the southern great plains, *Journal of Hydrometeorology*, *14*(3), 700–721.

Rauscher, S. A., E. Coppola, C. Piani, and F. Giorgi (2010), Resolution effects on regional climate model simulations of seasonal precipitation over Europe, *Climate Dynamics*, *35*(4), 685–711.

Rhoades, A. M., X. Huang, P. A. Ullrich, and C. M. Zarzycki (2015), Characterizing sierra nevada snowpack using variable-resolution cesm, *Journal of Applied Meteorology and Climatology*, (2015).

Sacks, W. J., B. I. Cook, N. Buenning, S. Levis, and J. H. Helkowski (2009), Effects of global irrigation on the near-surface climate, *Climate Dynamics*, *33*(2-3), 159–175.

Salas, W., P. Green, S. Frolking, and C. Li (2006), Estimating irrigation water use for california agriculture: 1950s to present, *Contract*, *603*, 862–0244.

Segal, M., Z. Pan, R. Turner, and E. Takle (1998), On the potential impact of irrigated areas in north america on summer rainfall caused by large-scale systems, *Journal of Applied Meteorology*, *37*(3), 325–331.

Shiklomanov, I. A. (2000), Appraisal and assessment of world water resources, *Water international*, *25*(1), 11–32.

Siebert, S., P. Döll, J. Hoogeveen, J.-M. Faures, K. Frenken, and S. Feick (2005), Development and validation of the global map of irrigation areas, *Hydrology and Earth System Sciences Discussions Discussions*, *2*(4), 1299–1327.

Siebert, S., P. Döll, S. Feick, J. Hoogeveen, and K. Frenken (2007), *Global Map of Irrigation Areas*, FAO Frankfurt, Germany.

Snyder, M., L. Kueppers, L. Sloan, D. Cavan, J. Jin, H. Kanamaru, N. Miller, M. Tyree, H. Du, and B. Weare (2006), Regional climate effects of irrigation and urbanization in the western united states: A model intercomparison, *Lawrence Berkeley National Laboratory.*

Solomon, S. (2007), *Climate change 2007-the physical science basis: Working group I contribution to the fourth assessment report of the IPCC*, vol. 4, Cambridge University Press.

Staniforth, A. N., and H. L. Mitchell (1978), A variable-resolution finite-element technique for regional forecasting with the primitive equations, *Monthly Weather Review*, *106*(4), 439–447.

Teixeira, E. I., G. Fischer, H. van Velthuizen, C. Walter, and F. Ewert (2013), Global hot-spots of heat stress on agricultural crops due to climate change, *Agricultural and Forest Meteorology*, *170*, 206–215.

Wilkinson, R., K. Clarke, J. Reichman, and J. Dozier (2002), Preparing for a changing climate: the potential consequences of climate variability and change for california, *Report for the US Global Change Research Program.*

Williams, A. P., R. Seager, J. T. Abatzoglou, B. I. Cook, J. E. Smerdon, and E. R. Cook (2015), Contribution of anthropogenic warming to california drought during 2012–2014, *Geophysical Research Letters.*

Zarzycki, C. M., C. Jablonowski, D. R. Thatcher, and M. A. Taylor (2015), Effects of localized grid refinement on the general circulation and climatology in the community atmosphere model, *Journal of Climate*, *28*(7), 2777–2803.

Corresponding author: Xingying Huang, Department of Land, Air and Water Resources, University of California Davis, Davis, CA 95616, USA. (xyhuang@ucdavis.edu)

Table 1. RMSD, MSD and Corr of Tmax between models and observations over CV in JJA from 1980-2005.

JJA	UW			PRISM		
	RMSD	MSD	Corr	RMSD	MSD	Corr
NRG	1.809	1.003	0.999	1.824	1.005	0.999
IRG	1.511	-0.357	0.999	1.422	-0.355	0.999
IRG(0.5)	1.467	-0.205	0.999	1.383	-0.203	0.999

Notes: RMSD (root-mean-square deviation) = $\sqrt{\frac{1}{N}\sum_{i=1}^{N}(v_i - \hat{v}_i)^2}$, MSD (mean signed difference) = $\frac{1}{N}\sum_{i=1}^{N}(v_i - \hat{v}_i)$, and Corr (Spatial correlation) is assessed by computing Pearson product-moment coefficient of linear correlation.

Table 2. Values of multiple variables over CV from models in JJA from 1980-2005.

	2m specific humidity* (g/kg)	Sensible heat flux* (W/m^2)	10m wind* (m/s)	Latent heat flux* (W/m^2)	Precipitation (mm/day)	Irrigated water* (mm/day)	Surface runoff* (mm/day)	Ground evaporation* (mm/day)	Soil moisture* kg/m^2
NRG	6.994	123.211	3.061	36.563	0.107	0.000	0.015	0.163	75.582
IRG	7.852	104.752	2.913	62.574	0.119	2.838	1.610	0.907	79.439
IRG(0.5)	7.782	105.730	2.926	61.695	0.118	1.272	0.236	0.892	78.366

Table 3. The first four moments of the JJA Tmax frequency for models and observations over CV. Column titles refer to the Average (Avg), Variance (Var), Skewness (Skew) and Kurtosis (Kurt).

	Avg	Var	Skew	Kurt
NRG	33.735	27.502	-0.417	0.234
IRG	32.374	21.343	-0.505	0.415
IRG(0.5)	32.537	21.125	-0.556	0.632
UW	32.745	22.442	-0.717	0.794
PRISM	32.814	24.007	-0.802	1.120

Notes: If skew > 0 [skew < 0], the distribution trails off to the right [left]. If kurtosis > 0 [< 0], a sharper [flatter] peak compared to a normal distribution (leptokurtic and platykurtic, respectively) is expected.

Table 4. The mean hot spell features for models and UW observation over CV in JJA from 1980-2005.

	NRG	IRG	IRG(0.5)	UW
Hot spell length	9.637	7.014	6.483	6.930
Hot spell number	2.220	1.500	1.505	1.539
Tmax	40.496	39.806	39.887	39.720

change the order of variables

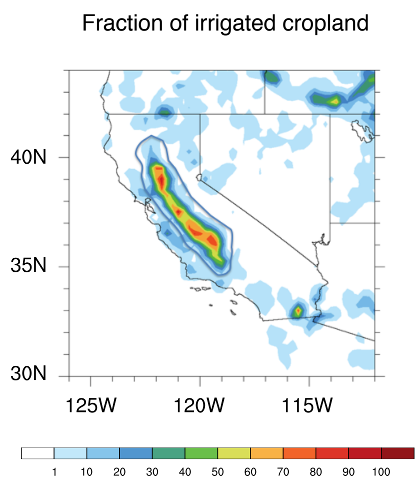

Figure 1. The fraction of irrigated cropland at each grid cell (unit: %) (Blue line is the boundary of the CV region.).

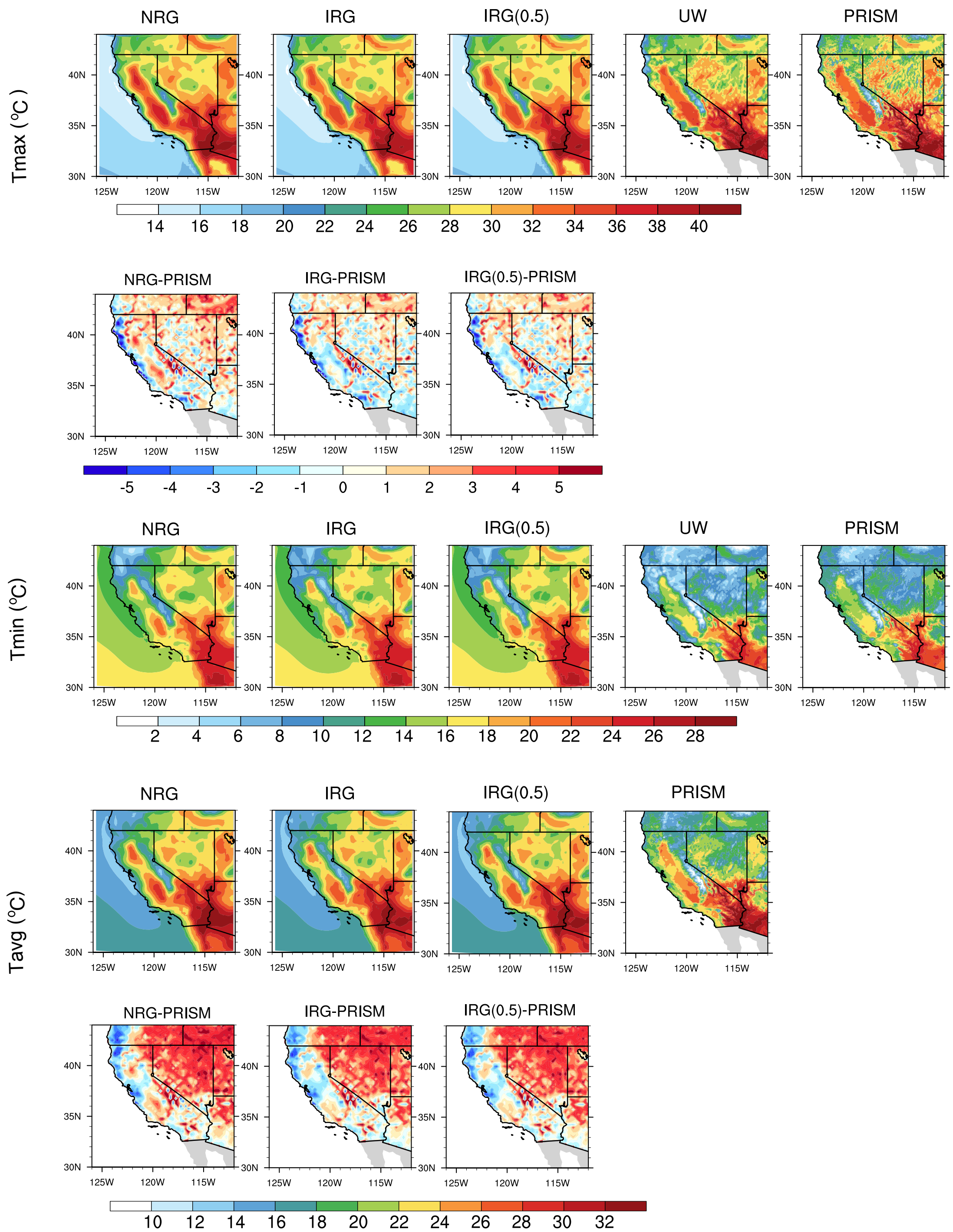

Figure 2. Average JJA Tmax, Tmin and Tavg over year 1980-2005 for models and observations (unit: °C).

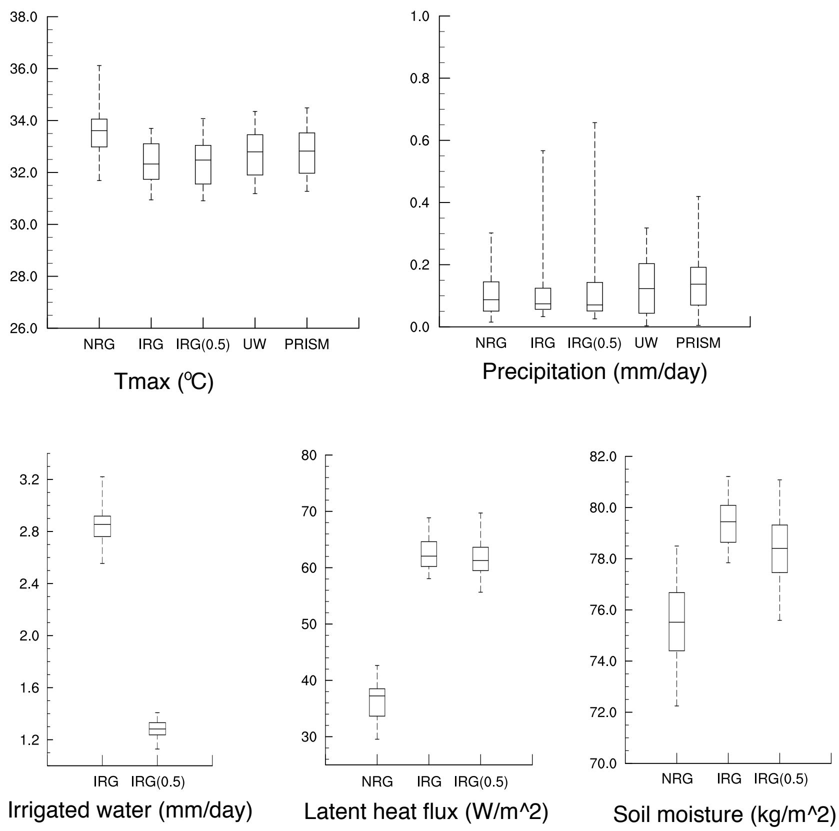

Figure 3. The boxplot for Tmax, Precipitation, irrigated water, latent heat flux and soil moisture. (From up to down, horizontal lines represent maximum, third quartile, median, first quartile and minimum respectively)

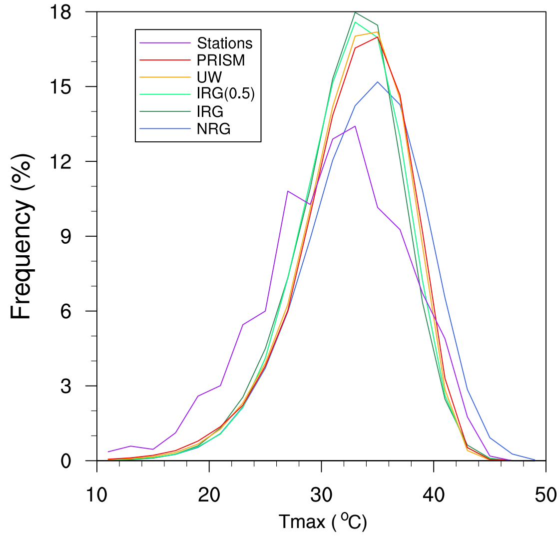
Stations
PRISM
UW
IRG(0.5)
IRG
NRG
Frequency (%)
Tmax (^{o}C)
0
3
6
9
12
15
18
10
20
30
40
50

Figure 4. .

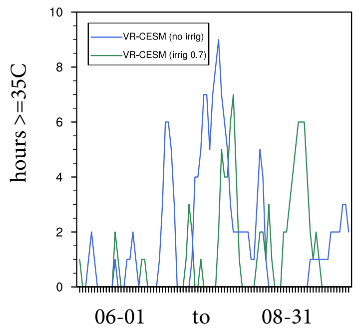

10
8
6
4
2
0
hours >=35C
VR-CESM (no irrig)
VR-CESM (irrig 0.7)
06-01
to
08-31

Figure 5. .

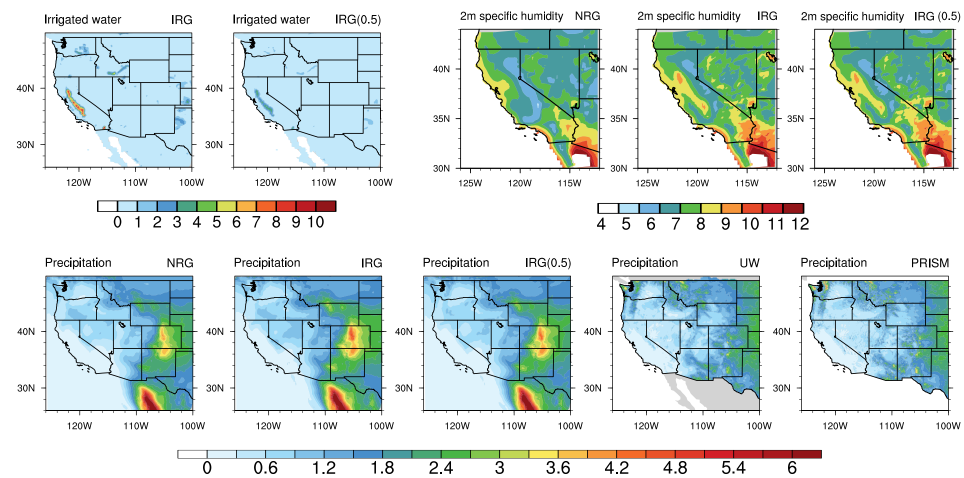
Irrigated water IRG
Irrigated water IRG(0.5)
2m specific humidity NRG
2m specific humidity IRG
2m specific humidity IRG (0.5)
0 1 2 3 4 5 6 7 8 9 10
4 5 6 7 8 9 10 11 12
Precipitation NRG
Precipitation IRG
Precipitation IRG(0.5)
Precipitation UW
Precipitation PRISM
0 0.6 1.2 1.8 2.4 3 3.6 4.2 4.8 5.4 6

a

Figure 6. .